COLD SPRING HARBOR
Molecular Case Studies

RESEARCH REPORT

A novel variant in *DYNC1H1* could contribute to human amyotrophic lateral sclerosis-frontotemporal dementia spectrum

Alexios-Fotios A. Mentis,[1,2,3,4] Dimitrios Vlachakis,[2,5,6] Eleni Papakonstantinou,[5] Ioannis Zaganas,[7,8] George P. Patrinos,[9,10,11] George P. Chrousos,[2] and Efthimios Dardiotis[4]

[1]Public Health Laboratories, Hellenic Pasteur Institute, Athens 115 21, Greece; [2]University Research Institute of Maternal and Child Health & Precision Medicine, and UNESCO Chair on Adolescent Health Care, [3]Medical School, National and Kapodistrian University of Athens, "Aghia Sophia" Children's Hospital, Athens 115 27, Greece; [4]Laboratory of Neurogenetics, Department of Neurology, School of Medicine, University Hospital of Larissa, University of Thessaly, Larissa 413 34, Greece; [5]Laboratory of Genetics, Department of Biotechnology, School of Applied Biology and Biotechnology, Agricultural University of Athens, Athens 118 55, Greece; [6]Division of Endocrinology and Metabolism, Center of Clinical, Experimental Surgery and Translational Research, Biomedical Research Foundation of the Academy of Athens, Athens 115 27, Greece; [7]Neurogenetics Laboratory, Medical School, University of Crete, Heraklion, Crete 715 00, Greece; [8]Neurology Department, University Hospital of Crete, Heraklion, Crete 715 00, Greece; [9]Department of Pharmacy, University of Patras School of Health Sciences, Patras 265 34, Greece; [10]Department of Pathology, College of Medicine and Health Sciences, [11]Zayed Center of Health Sciences, United Arab Emirates University, Al-Ain 155 51, United Arab Emirates

Abstract Amyotrophic lateral sclerosis (ALS) belongs to the ALS-frontotemporal dementia (FTD) spectrum and is hallmarked by upper and lower motor neuron degeneration. Here, we present a patient with a cytoplasmic dynein 1 heavy chain 1 (*DYNC1H1*) pathogenic variant who fulfilled the ALS El Escorial criteria, and we review relevant literature. Using whole-exome sequencing, we identified a deleterious point variant in *DYNC1H1* (c.4106A > G (p. Q1369R)) as a likely contributor to the ALS phenotype. In silico structural analysis, molecular dynamics simulation, and protein stability analysis predicted that this variant may increase DYNC1H1 protein stability. Moreover, this variant may disrupt binding of the transcription factor TFAP4, thus potentially acting as duon. Because (a) DYNC1H1 forms part of a ubiquitous eukaryotic motor protein complex, and (b) disruption of dynein function by perturbation of the dynein–dynactin protein complex is implicated in other motor neuron degenerative conditions, this variant could disrupt processes like retrograde axonal transport, neuronal migration, and protein recycling. Our findings expand the heterogenous spectrum of the *DYNC1H1* pathogenic variant–associated phenotype and prompt further investigations of the role of this gene in ALS.

Corresponding author:
amentis1@jhu.edu

Ontology term: amyotrophic lateral sclerosis

Published by Cold Spring Harbor Laboratory Press

doi:10.1101/mcs.a006096

[Supplemental material is available for this article.]

INTRODUCTION

Amyotrophic lateral sclerosis (ALS)-frontotemporal dementia (FTD) spectrum disorders represent a group of rare and heterogeneous neurodegenerative diseases presenting with symptoms such as frontotemporal dementia, primary lateral sclerosis, progressive muscular

atrophy, and pseudobulbar palsy (de Vries et al. 2019; Abramzon et al. 2020). In Europe, the incidence of ALS is around two to three cases per 100,000 individuals (Rooney et al. 2017), whereas the prevalence is expected to increase by 2040, most likely because of an aging population. Thus, the socioeconomic disease burden is expected to increase in the coming decades (Arthur et al. 2016).

ALS is clinically hallmarked by the rapid deterioration of spasticity and muscle wasting, leading to death due to insufficiency of respiratory muscles, and pathologically by the loss of motor neurons in the central nervous system (Pampalakis et al. 2019). Heterogenous initial clinical manifestation of the disease has been noted among afflicted patients (Hardiman et al. 2017). Despite the initial descriptions of the disease in the nineteenth century, the complete etiology of ALS is not yet fully deciphered (Connolly et al. 2015). Among ALS cases, 10% are familial, whereas the remaining are considered sporadic. Pathogenic variants of around 20 genes explain most familial cases; however, they can only explain ~10% of sporadic cases (Chen et al. 2013). In every case, the degree of genetic contribution seems to vary from typical Mendelian patterns to epistatic associations of rare variants, along with the influence of environmental factors and cellular stochastic events (Talbot et al. 2018). In familial types of ALS, most of the implicated genes are not entirely penetrant, and the phenotype is, in general, not dependent on the genotype (Al-Chalabi et al. 2017). Several pieces of evidence support an oligogenic basis for ALS (Keogh et al. 2018; Lattante et al. 2019). However, the implications of genetic classification on diagnosis, treatment, and prognosis of patient outcomes are still unexplored, with polygenic risk scores only recently developed (Bandres-Ciga et al. 2019).

Among ALS-related genes, the genes encoding superoxide dismutase-1 (*SOD1*), Chromosome 9 open reading frame 72 (*C9orf72*), and transactive response DNA binding protein 43 kDa (*TARDBP*) are the most commonly mutated ones (Wegorzewska et al. 2009; Chia et al. 2018; Sokratous et al. 2020), whereas less common genes include those encoding RNA-binding proteins and expansions of oligonucleotide repeats (Corrado et al. 2011; Kapeli et al. 2017). Genes encoding cytoskeleton proteins, such as dynactin and tubulin, have also been linked to ALS pathology (LaMonte et al. 2002; Helferich et al. 2018). Pathogenic variants in the dynein/dynactin complex have been implicated in ALS pathology in mouse models (LaMonte et al. 2002; Hafezparast et al. 2003; Courchesne et al. 2011). Pathogenic variants in the human dynein cytoplasmic 1 heavy chain 1 gene (*DYNC1H1*), which encodes a major subunit of the cytoplasmic dynein1 complex, have been associated with several neurological, neurodevelopmental, and motor neuron diseases (Al-Chalabi et al. 2014) but have yet to be implicated in ALS.

Herein, following similar studies assessing monogenic and polygenic traits in neurological and neuropsychiatric conditions (Ayalew et al. 2012; Talkowski et al. 2012; Claussnitzer et al. 2015) and building upon previous major studies (Amabile et al. 2020), we report on the potential contribution of a deleterious *DYNC1H1* variant to the ALS phenotype of a late Caucasian patient who presented with respiratory insufficiency as the earliest manifestation and with depression and benign prostatic hyperplasia as comorbidities. In addition, we review the literature regarding phenotypes related to *DYNC1H1* pathogenic variants.

RESULTS

Clinical Presentation and Family History

A 61-yr-old, Caucasian male (of Greek origin) with no known family history of ALS or other neurological disorder presented initially with respiratory manifestations. He was ultimately diagnosed with ALS and treated with riluzole. Past medical history, initial assessment for the disease of interest, follow-up sequalae, and laboratory findings are presented in

Supplemental Tables S1 and S2. Despite the initial improvement of his clinical manifestations, he progressively deteriorated and died in January 2018.

Several factors indicated the likelihood of a motor neuron disorder: the progressive course of the disease (lasting 6 mo), episodes of respiratory failure, and compatible electromyogram (EMG) results. No sign or evidence of a reversible motor neuron disorder was present following full clinical and laboratory evaluation, leading to a diagnosis of definite ALS in alignment with the El Escorial criteria (Carvalho and Swash 2009). No diagnostic challenge in terms of financial, language, or cultural barriers existed. Although the diagnosis of ALS was supported by the neurological and neurophysiological examination and by muscle biopsy showing multiple grouped round atrophic and regenerating muscle fibers (group atrophy), certain features extended beyond the typical clinical presentation often observed in patients with motor neuron disease. Despite the patient's vague complaints of fatigue and dyspnea, no specific EMG findings were reported by the neurologists who first examined him in the ambulatory setting. At that point, the patient had no clinical signs of twitching or atrophy during physical examination. Perplexingly, after ~2 mo from the initial examination, he presented with severe muscle atrophy, respiratory insufficiency, frequent muscle twitching, and spontaneous activity in the EMG. The patient's ALS course, including respiratory failure to a degree severe enough to require artificial ventilation in the intensive care unit, followed by the gradual improvement of respiratory function, is a rare manifestation of the disease.

Clinical and laboratory findings excluded diagnoses differential to ALS such as non-ALS neuromuscular mimic disorders, chronic inflammatory demyelinating neuropathy, acquired neuromyotonia, myopathy, Kennedy disease, myasthenia gravis, axonal neuropathy, multifocal motor neuropathy, spinal muscular atrophy, Hirayama disease, distal hereditary motor neuronopathy with pyramidal features, facial onset sensory and motor neuropathy syndrome, cervical radiculopathy, lead toxicity, post-polio syndrome, space-occupying lesions of the esophagus, sarcoidosis, polymyositis, multifocal motor neuropathy, flail arm syndrome, lesions of the brachial plexus, cervical radiculopathies, and distal myopathies seeming like leg-onset ALS (or neuropathies). Perry syndrome was also considered as a differential diagnostic option because of the coexisting depression and respiratory insufficiency but was excluded because (a) respiratory insufficiency can (although rarely) be the first manifestation of ALS, whereas depression is a quite common disease, which can coexist with ALS exactly because of its commonality; and (b) in alignment with the established criteria for Perry syndrome's diagnosis (Mishima et al. 2018), amyotrophy contrasts Perry syndrome's diagnosis, whereas clinical signs or family history of parkinsonian features or respiratory insufficiency were absent from our case.

Genomic Analysis

Based on the working diagnosis of ALS and the lack of a known familial ALS basis for this patient (as neither the deceased parent nor all living relatives suffered from ALS), we analyzed 14 genetic candidates including *C9orf72*, *PRF1*, *TDP43*, and *DYNC1H1* (Supplemental Materials and Methods). Of major interest was a heterozygous variant in *DYNC1H1* (c.4106A > G (p.Q1369R), transcript ID NM_001376.5), ranked 48th among the top 100 variants prioritized by eDiva (Table 1). Functionally, the p.Q1369R pathogenic variant was classified as a variant of unknown significance, suggesting its potential relevance to the clinical phenotype of the patient. Moreover, the variant was not reported in healthy individuals according to the major databases of genetic variation (ExAC, 1000 Genomes, Exome Variant Server), which also include information on the Greek population. Considering the association of other *DYNC1H1* variants with other types of motor neuron disease (Hafezparast et al. 2003; Scoto et al. 2015), as well as the association of its sister protein dynactin with human ALS (Moore et al. 2009), we further examined the potential contribution of this gene mutation to our patient's ALS genetic background.

Table 1. *DYNC1H1* variant information

Gene	Chromosome	HGVS DNA reference	HGVS protein reference	Variant type	Predicted effect	dbSNP/dbVar ID	Genotype	Parent of origin	Comments	Sequencing coverage
DYNC1H1	14	NM_001376: c.A4106G	p.Q1369R	Missense	Substitution	NA	Heterozygous	Parental genotypes are not available. Possible de novo variant.	The variant has not been reported to date in any major databases of genetic variation (e.g., gnomAD).	The variant displayed a high sequencing depth of 135 reads, of which 59 supported the reference allele and 76 supported the alternate allele, with no evidence of strand bias.

(HGVS) Human Genome Variation Society, (dbSNP) Single Nucleotide Polymorphism Database, (dbVar) Database of Structural Variation, (NA) not applicable, (gnomAD) Genome Aggregation Database.

In Silico Analysis of the *DYNC1H1* Variant

Two images depicting the genomic region surrounding the candidate variant at low (2.3-kb window) and high (131-bp window) resolution are provided in Supplemental Figure S1. Variant review in the Integrative Genomics Viewer (IGV) showed that the region surrounding the variant was free from deletions and insertions, and there was no evidence of excessive variation rate. The variant displayed a high sequencing depth of 135 reads, of which 59 supported the reference allele and 76 supported the alternate allele, with no evidence of strand bias. Reads overlapping the variant displayed high mapping quality (MQ = 60; >40 is acceptable) and no bias in read MQ between the reads supporting reference and alternate alleles (MQRankSum = 1.305, >−12.5 is acceptable) (McKenna et al. 2010). Similarly, the base quality score for the variant bases was 37 for most reads (>30 is good quality) (Ewing and Green 1998). Finally, the variant did not show any bias toward read ends (ReadPosRankSum = −0.909, >−8 is acceptable). Overall, the variant quality control indicated that the candidate variant was a bona fide variant.

Table 2 lists the damage and conservation scores and their corresponding quantiles for the *DYNC1H1* variant. Caution was applied while interpreting these findings, as some of the applied tools proposed a cutoff at which a variant was either benign or damaging. Quantiles are provided to normalize for the different score thresholds used by different scoring methods (e.g., both PolyPhen-2 and CADD placed the p.Q1369R variant in the 98.9% quantile despite differentially ranking the variant by score).

Multiple protein alignment of the affected *DYNC1H1* locus across species revealed that the locus is highly conserved (Fig. 1) in invertebrates but not in *Dictyostelium discoideum* and *Saccharomyces cerevisiae* (which harbors the same residue, R, as the variant).

Comparative Analysis of Reported *DYNC1H1* Variants

The p.Q1369R variant maps to the dynein heavy chain, amino-terminal region 2 domain. Although no specific function has been assigned to this domain (http://www.ebi.ac.uk/interpro/entry/IPR013602), it forms part of the tail linking the amino-terminal region,

Table 2. Damage and conservation scores and their quantiles for the p.Q1369R *DYNC1H1* variant

	Score	Quantile
Damage scores		
SIFT	0.28	96.25
PolyPhen-2	0.34	98.90
MutAss	1.32	98.71
Condel	0.49	97.60
CADD	22.1	98.89
Eigen	3.56	99.48
Conservation scores		
GERP++	5.85	99.76
PhyloP		
Mammals	2.23	99.05
Primates	0.46	87.64
Vertebrates	5.17	99.83
PhastCons		
Mammals	1	100
Primates	0.91	96.01
Vertebrates	0.91	96.01

(SIFT) Sorting Intolerant From Tolerant, (PolyPhen-2) Polymorphism Phenotyping v2, (MutAss) Mutation Assessor, (Condel) Consensus Deleteriousness, (CADD) Combined Annotation Dependent Depletion, (GERP++) Genomic Evolutionary Rate Profiling, (PhyloP) phylogenetic P-values, (PhastCons) Phylogenetic Analysis with Space/Time Models (PHAST).

responsible for dimerization and cargo binding, with the carboxy-terminal portion, responsible for motor activity and microtubule binding (Oiwa and Sakakibara 2005). Figure 2 delineates the major domains of *DYNC1H1* and maps the p.Q1369R pathogenic variant, as well as previously reported *DYNC1H1* variants associated with various pathologies (Niu et al. 2015; Hoang et al. 2017). The figure also maps two pathogenic variants in mouse models, p.F582Y and p.Y1057C (Hoang et al. 2017).

DYNC1H1 variants have been linked to several neurological and motor neuron pathologies of differing severity levels—for example, they have been recently linked to upper and lower motor neuron anomalies (Viollet et al. 2020), overlapping neurodevelopmental and neuromuscular phenotypes (Becker et al. 2020), and other intermixed phenotypes (Amabile et al. 2020) (for further review, see Supplemental Tables S5 and S6). Our patient displayed a late-onset pathology. In this context, we compared the predicted functional impact of the *DYNC1H1* variant with that of previously reported variants (Hoang et al. 2017). Based on damage and conservation scores, as well as multifeature ranking, the novel p.Q1369R *DYNC1H1* variant appeared to have a more moderate impact than that of previously reported *DYNC1H1* variants (Table 3).

Effect of the *DYNC1H1* Variant on miRNA Recognition Sequences, Splicing Sites, and Transcription Factor Binding Motifs

To assess the possible effects of *DYNC1H1* variant on miRNA recognition sites, we used the miRcode database (Jeggari et al. 2012) to search for miRNA targets within the coding regions of *DYNC1H1*. The closest miRNA target (miR-338/338-3p) was located 173 bp away from the point pathogenic variant; therefore, the *DYNC1H1* variant was considered unlikely to affect annotated miRNA target sites.

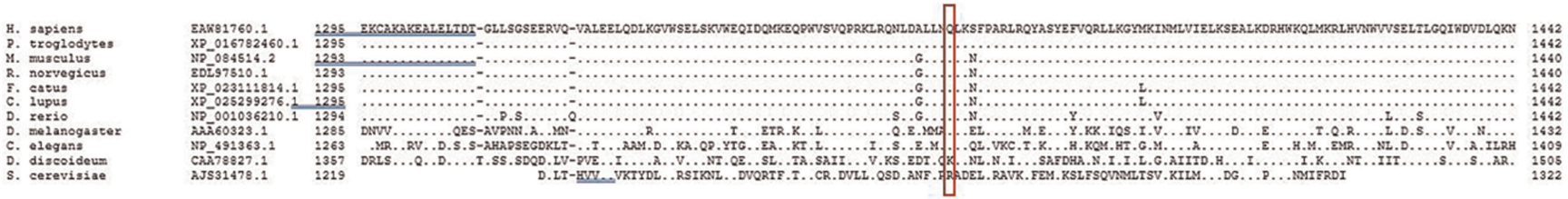

Figure 1. Multiple protein alignment of the affected *DYNC1H1* locus across different species.

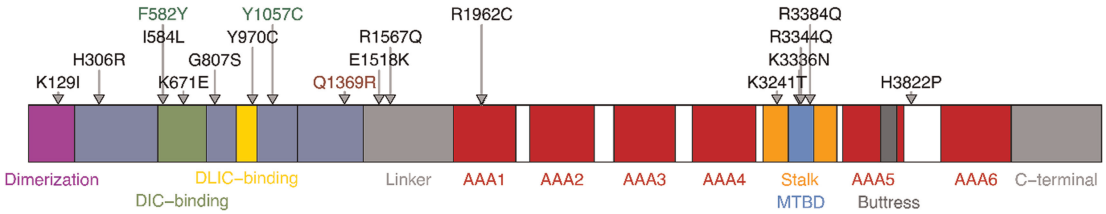

Figure 2. DYNC1H1 protein domains and mapping of the novel Q1369R and previously reported pathogenic variants. The previous variants were assayed for functionality based on an in vitro dynein–dynactin-BICD2N motility assay measuring mechanochemical properties of the complex (Hoang et al. 2017). The R1962C and H3822P variants associated with malformations in cortical development (MCDs) exhibited significantly defected processivity and microtubule gliding (Hoang et al. 2017). Seven other variants also associated with MCD, K129I, K3336N, R3344Q, R3384Q, E1518K, R1567Q, and K3241T, demonstrated either reduced processivity or both reduced processivity and travel distance of the complex (Hoang et al. 2017). Four variants associated with spinal muscular atrophy with lower extremity predominance (SMALED) exhibited reduced complex travel distance, with the exception of the last variant: H306R, I584L, Y970C, and K671E. The F582Y and Y1057C variants identified in mice also showed reduced complex travel distance (Hoang et al. 2017). The G807S variant was identified to be associated with SMALED in a case report (Niu et al. 2015). (DIC) Disseminated intravascular coagulation, (MTBD) microtubule-binding domain.

The nearest exon–intron junction edge is located 30 bp upstream of the point pathogenic variant, whereas the downstream junction is 79 bp away. Thus, we postulated that the *DYNC1H1* variant is unlikely to interfere with splicing.

To evaluate whether the variant may affect any known transcription factor binding site (TFBS), we searched the JASPAR database (Sandelin et al. 2004) and identified the TFBS motif of TFAP4 (JASPAR ID MA0691.1) overlapping the variant (Supplemental Table S7). The variant position in TFAP4 motif had 100% frequency of reference allele, indicating a strong disruption potential (Fig. 3; Supplemental Table S7). We also manually checked the TFAP4 motif in the HOCOMOCO database (version 11) (http://hocomoco11.autosome.ru/motif/TFAP4_HUMAN.H11MO.0.A) (Kulakovskiy et al. 2016). We confirmed that only the reference, and not the alternate allele, matched the TFAP4 motif, corresponding to a maximum binding disruption score, similar to that in the JASPAR database.

Predicted Structural Effects of the DYNC1H1 p.Q1369R Pathogenic Variant

To predict the effect of the p.Q1369R variant on DYNC1H1 protein stability, we used I-Mutant2.0 (Capriotti et al. 2005) and MUpro (Cheng et al. 2006). MUpro results were of low confidence (confidence score, 0.62) and, thus, were not considered further. I-Mutant2.0 predicted an increased stability of the p.Q1369R DYNC1H1 protein (Supplemental Fig. S2); the index equaled 0, which, in turn, means that the prediction is not reliable (considering that, in general, the reliability index ranges from 0 to 10, with 10 being the highest reliability). We also used STRUM (Quan et al. 2016) to predict the effect of the p.Q1369R change on the protein structure. STRUM predicted a ddG value of 2.93 for Q-to-R transition, indicating increased protein stability. Figure 4A,B visualizes the affected residue (yellow) in its immediate context (blue) in low and high resolution, respectively. Phyre2 was unable to model the area including the affected residue (Fig. 4C,D).

Following similar approaches in other settings (Vlachakis 2009; Dror et al. 2012; Lesgidou et al. 2018; Goulielmos et al. 2019; Galdadas et al. 2020), we conducted molecular dynamics modeling to assess the *DYNC1H1* variant's effects on the corresponding protein. Dynein was modeled initially with the wild-type sequence bearing a glutamine residue at position 1369. The X-ray structure of the functional full-length dynein motor domain (Protein Data Bank ID:

Table 3. Damage and conservation scores and their quantiles for the novel (p.Q1369R) and the previously reported *DYNC1H1* variants

	Damage scores											
	SIFT		PolyPhen-2		MutAss		Condel		CADD		Eigen	
Variant	Score	Quantile	Score	Quantile	Score	Quantile	Score	Quantile	Score	Quantile	Score	Quantile
p.H3822P	0.00	99.34	0.99	99.78	2.94	99.85	0.59	98.64	26.40	99.74	11.76	99.97
p.Y1057C	0.00	99.34	0.98	99.67	3.06	99.87	0.69	99.11	28.80	99.85	11.92	99.98
p.R1962C	0.00	99.34	1.00	100.00	4.612	100.00	0.643	98.89	35.00	99.98	12.63	99.98
p.E1518K	0.00	99.34	0.99	99.88	2.51	99.73	0.573	98.51	34.00	99.96	10.90	99.97
p.F582Y	0.00	99.34	1.00	100.00	3.49	99.93	0.68	99.07	27.30	99.79	12.34	99.98
p.R1567Q	0.01	99.01	0.99	99.74	2.99	99.86	0.63	98.85	34.00	99.96	10.940	99.97
p.K3241T	0.04	98.50	0.76	99.31	2.38	99.67	0.60	98.70	29.00	99.86	6.85	99.86
p.I584L	0.02	98.81	0.91	99.50	3.07	99.87	0.59	98.64	25.90	99.70	6.9245	99.87
p.K3336N	0.01	99.01	0.95	99.58	3.18	99.89	0.69	99.11	29.10	99.86	7.68	99.90
p.R3384Q	0.01	99.01	0.74	99.29	3.42	99.92	0.68	99.06	33.00	99.94	8.04	99.91
p.Y970C	0.02	98.81	0.78	99.33	2.69	99.79	0.63	98.84	25.20	99.62	4.62	99.68
p.H306R	0.19	97.01	0.06	98.22	1.91	99.33	0.462	97.07	17.77	98.07	2.99	99.31
p.K671E	0.75	92.75	0.06	98.22	1.76	99.17	0.47	97.24	12.52	94.49	2.50	99.13
p.R3344Q	0.11	97.76	0.07	98.26	2.32	99.64	0.62	98.76	24.80	99.57	5.00	99.72
p.G807S	0.30	96.05	0.10	98.41	1.289	98.67	0.47	97.29	21.20	98.76	3.04	99.33
p.K129I	0.15	97.40	0.99	99.78	1.99	99.41	0.43	96.29	14.00	95.97	6.00	99.81
p.Q1369R	0.28	96.24	0.34	98.90	1.32	98.70	0.49	97.60	22.10	98.89	3.55	99.48

(*Continued*)

Table 3. *Continued*

	Conservation scores													
			PhyloP						PhastCons					
	GERP++		Mammals		Primates		Vertebrates		Mammals		Primates		Vertebrates	
Variant	Score	Quantile	Score	Quantile	Score	Quantile	Score	Quantile	Score	Quantile	Score	Quantile	Score	Quantile
p.H3822P	5.82	99.74	2.23	99.03	0.53	93.29	5.16	99.82	1.000	100.00	0.87	95.34	1.0	100.0
p.Y1057C	5.73	99.61	2.19	98.93	0.46	86.20	5.12	99.81	1.000	100.00	0.99	99.09	1.0	100.0
p.R1962C	4.31	96.75	2.64	99.69	0.65	98.00	2.03	96.35	1.000	100.00	0.99	99.55	1.0	100.0
p.E1518K	5.70	99.57	2.70	99.76	0.66	100.00	6.07	99.97	0.99	97.01	0.99	99.09	1.0	100.0
p.F582Y	5.85	99.76	2.23	99.03	0.53	93.29	5.17	99.83	0.99	96.51	0.93	96.54	1.0	100.0
p.R1567Q	4.88	98.21	1.45	97.42	0.66	100.00	4.57	99.67	0.99	95.77	0.99	98.99	1.0	100.0
p.K3241T	5.63	99.48	2.14	98.83	0.53	91.44	5.08	99.81	0.99	97.41	0.99	99.19	1.0	100.0
p.I584L	5.85	99.76	2.23	99.03	0.53	93.29	5.17	99.83	0.99	96.71	0.88	95.46	1.0	100.0
p.K3336N	4.60	97.54	2.64	99.69	0.47	88.65	2.99	98.39	1.000	100.00	0.99	98.99	1.0	100.0
p.R3384Q	4.56	97.44	1.31	96.81	0.47	88.65	4.12	99.48	0.99	97.01	0.76	93.90	1.0	100.0
p.Y970C	4.71	97.83	1.03	95.36	0.30	39.24	3.30	98.85	0.80	92.40	0.85	95.02	1.0	100.0
p.H306R	5.24	98.88	2.10	98.74	0.50	89.58	4.99	99.78	0.97	94.92	0.99	98.57	1.0	100.0
p.K671E	5.61	99.44	2.14	98.81	0.53	93.29	5.07	99.80	1.000	100.00	0.78	94.14	1.0	100.0
p.R3344Q	5.36	99.07	2.53	99.53	0.47	88.65	6.02	99.96	0.86	92.93	0.99	99.68	0.99	91.7
p.G807S	5.52	99.30	2.77	99.86	0.66	100.00	6.18	99.98	0.95	94.17	0.76	93.88	1.0	100.0
p.K129I	5.68	99.55	2.17	98.89	0.40	84.43	4.77	99.73	0.99	95.59	0.023	65.57	1.0	100.0
p.Q1369R	5.85	99.76	2.23	99.04	0.46	87.63	5.17	99.83	1.00	100.00	0.91	96.01	1.0	100.0

(SIFT) Sorting Intolerant From Tolerant, (PolyPhen-2) Polymorphism Phenotyping v2, (MutAss) Mutation Assessor, (Condel) Consensus Deleteriousness, (CADD) Combined Annotation Dependent Depletion, (GERP++) Genomic Evolutionary Rate Profiling.

Figure 3. The *DYNC1H1* variant is predicted to disrupt binding of the transcription factor TFAP4. Sequence alignments with the TFAP4 motif are shown. (*Top*) Reference and alternate sequence alignments with the TFAP4 motif shown in red (5′ to 3′). (*Bottom*) Consensus motif logo for TFAP4 obtained from the JASPAR core vertebrate database.

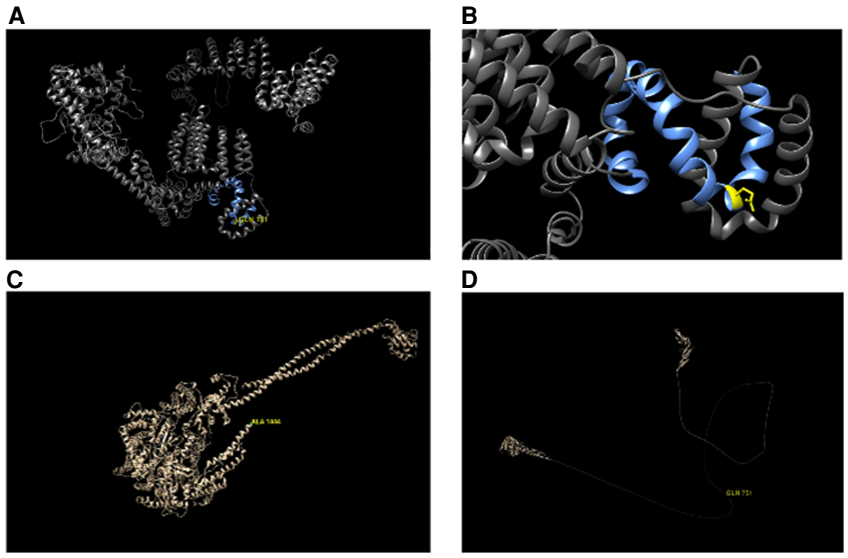

Figure 4. Homology modeling using STRUM and Phyre2. (*A*) Visualization of the region surrounding the *DYNC1H1* variant at low resolution. (*B*) Region surrounding the *DYNC1H1* variant at high resolution. (*C*) Structure modeling with Phyre2 in normal mode for the first 3500 amino acids. Phyre2 was unable to model the first 1443 amino acids. (*D*) Structure modeling with Phyre2 in intensive mode for the 1500 amino acids centered on the residue affected by the candidate variant. Phyre2 was unable to model the mid region from amino acid 301 to 659.

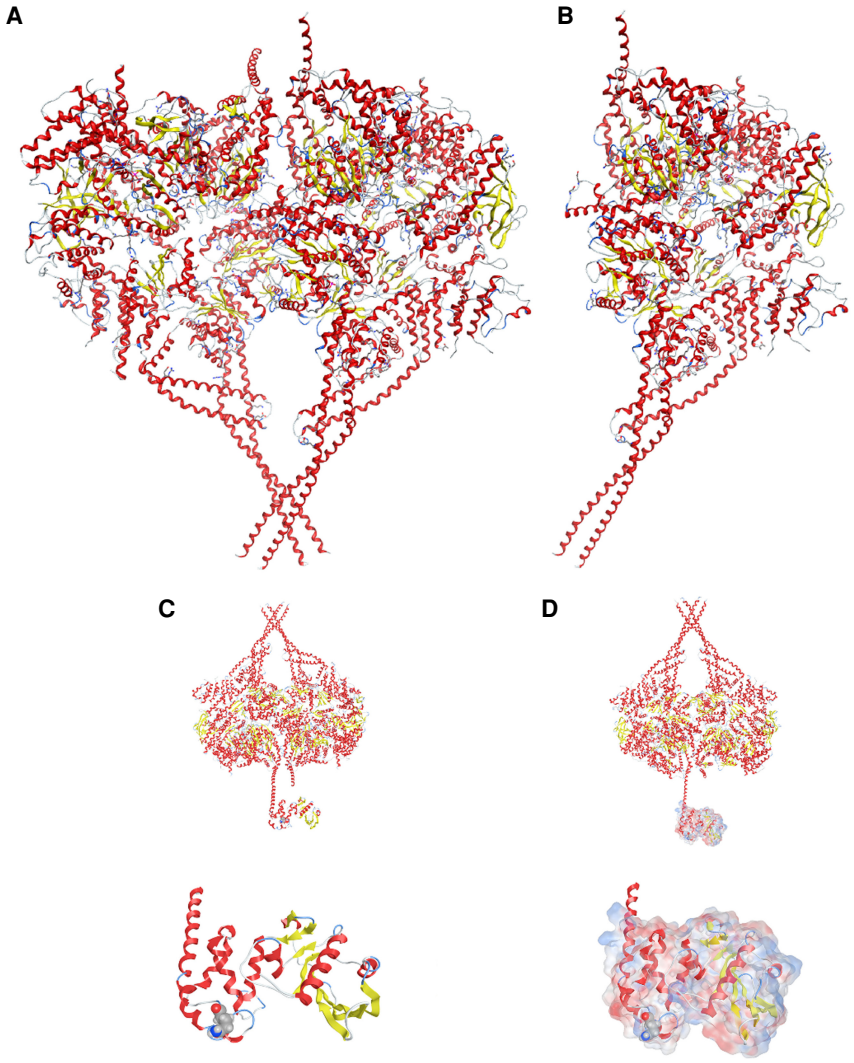

Figure 5. Molecular dynamics modeling. (*A*) The X-ray structure of the functional full-length dynein motor domain from Protein Data Bank (ID: 3VKH). (*B*) Modeling on the functional full length of the dynein motor domain to construct the noncrystalized part. (*C*) (*Top*) The dynein X-ray structure with the modeled missing part. (*Bottom*) Zoom-in of the modeled part. (*D*) Same as *C* but with electrostatic surface potential (red to blue represents negative to positive).

3VKH) has not been fully crystalized, and the mutated amino acid is located in this noncrystalized part (Fig. 5A). Therefore, the X-ray structure of dynein was enhanced with its missing part by applying conventional homology modeling techniques and ab initio calculations. Molecular dynamics simulations were then applied to the full modeled dynein molecular system to allow it to relax conformationally and, thus, to energetically optimize it. The position of residue 1369 lies on an α-helix located in the outer part of the model; more specifically, the side chain of both the wild-type and mutant p.Q1369 residues seemed to protrude well into the solvent (Fig. 5B). However, no further modeling-based estimations on potential interactions with other proteins could be made, thus allowing no further conclusions on whether the stability is increased or decreased.

DISCUSSION

We reported on a patient with a unique profile of potential ALS-related gene variants. Sporadic ALS caused by multigene variants is associated with a disease onset that is 10 yr earlier than that of familiar ALS caused by a single-gene mutation (Kenna et al. 2013; Cady et al. 2015; McCann et al. 2021). The rare *DYNC1H1* variant in our study could be a potential contributor to the genetic profile of this patient, possibly in combination with the variants in *CCDC88C*, *PRKCG*, *DMXL2*, *SPTLC1*, and *SH3TC2*, as these variants have not been empirically ruled out (Supplemental Materials and Methods).

The current evidence is only suggestive of the role of the p.Q1369R variant in ALS in our patient, and further experiments are required to demonstrate whether it alters protein structure and/or function. Nonetheless, the contribution of this variant to the genetic etiology of ALS is supported both by our in silico analysis and by a literature review.

a. D*YNC1H1* is implicated in other types of motor neuron disease (e.g., spinal muscular atrophy; Supplemental Tables S5 and S6) and in ALS mouse models (although specific pathogenic variants may be neuroprotective) (Fergani et al. 2011).
b. Our patient had concrete ALS symptoms and was heterozygous for p.Q1369R, which is consistent with a dominant mode of action for the variant, similar to that of other *DYNC1H1* variants in other conditions (Supplemental Tables S5 and S6; Harms et al. 2012; Tsurusaki et al. 2012).
c. p.Q1369R is a novel variant (not previously reported in the GnomAD version 2.1.1, 3.1.1, or TOPMed Bravo Freeze 8 databases).
d. There is evidence for (and, in no case, against) a potential important role of this *DYNC1H1* variant into ALS—that is, supporting evidence of pathogenicity based on (i) the PP3 criterion, which refers to multiple lines of computational evidence support a deleterious effect on the gene or gene product (conservation, evolutionary, splicing impact, etc.) and moderate evidence of pathogenicity based on the (ii) PM2 criterion, which refers to a variant absent from controls (or at extremely low frequency if recessive) in Exome Sequencing Project, 1000 Genomes, or ExAC considering that, in the above sources of population frequency data, this variant's frequency is <0.001% in terms of frequency, as well as not reported in the GeneMatcher database (data not shown) (for the above criteria, see Richards et al. 2015).

Of note, because the parents' genotypes were not available, we cannot conclude whether this was an inherited or de novo variant.

Dynein/dynactin pathogenic variants in evolutionarily lower animal models, such as *Drosophila melanogaster*, *Caenorhabditis elegans*, and *Danio rerio,* are linked to dysfunctional neuromuscular junction and locomotor defects (Koushika et al. 2004; Garrett et al. 2014; Bercier et al. 2019). In humans, *DYNC1H1* pathogenic variants affect the interaction between dynein-1, dynactin, and cargo adaptor complexes, the dysfunction of which may lead to neurological disorders (Hoang et al. 2017). The extensive length of motor neuron axons (up to ~1 m) is linked to the transport of multiple cargoes from the axons to the soma and vice versa, implying that even minor loss- or gain-of-function variants can lead to reduced motor neuron functions and diverse phenotypes from childhood to adulthood (Marzo et al. 2019). Also, pathogenic variants in *DYNC1H1*-interacting proteins, such as BICD2 (Peeters et al. 2015) and dynein axonemal assembly factors (e.g., c11orf70, ZYYND10, NADYX1C1), are implicated in ALS pathophysiology (Andres-Benito et al. 2019).

ALS pathogenic variants are divided in three categories: (a) those in cytoskeletal proteins leading to alterations in axonal transport, (b) those in proteins involved in

homeostasis, and (c) those in proteins involved in RNA homeostasis/trafficking (Tsai et al. 2017). Because DYNC1H1 is a microtubule-associated protein, the p.Q1369R variant probably belongs to the first category. Other pathogenic variants in *DYNC1H1* have been associated with Charcot–Marie–Tooth disease, Alzheimer's disease, and spinal muscular atrophy, lower extremity-predominant 1 (Supplemental Tables S5 and S6). A previous report suggested that *DYNC1H1* was not associated with sporadic ALS based on a tagged single-nucleotide polymorphism (SNP), case-control study (Shah et al. 2006). Although 16 SNPs were analyzed, the case and control sample size limited the detection of rare variants and their association with the disease (Shah et al. 2006). Recently, three variants were identified, all of which are located in the motor domain of DYNC1H1, but their significance in ALS disease progression remains uncertain (Tripolszki et al. 2019). Two novel variants, of which the K1395Q variant was predicted as likely pathogenic, were also recently identified (Scarlino et al. 2020). In addition, research in mice has shown variant effects on molecular function of the dynein complex and neuronal degeneration (LaMonte et al. 2002; Hafezparast et al. 2003; Koushika et al. 2004; Courchesne et al. 2011; Garrett et al. 2014; Bercier et al. 2019). These findings, together with our case study, further illustrate that the role of *DYNC1H1* in ALS cannot be overlooked.

Our in silico analysis suggested that the *DYNC1H1* pathogenic variants may disrupt binding of the transcription factor TFAP4 to the *DYNC1H1* gene (Stergachis et al. 2013); however, our findings should be interpreted with caution (Ambrosini et al. 2020). The method used to assess transcription factor binding does not estimate *biological relevance* because the xxCAGCTGxx motif is found in many protein coding sequences and not every motif is expected to be regulated by TFAP4. Additional experiments are required to confirm whether TFAP4 physiologically binds to *DYNC1H1* and to determine duon function.

According to our structural model, the variant mapped to amino-terminal region 2 domain, which is structurally unsolved but thought to protrude away from other dynein subunit binding sites (Lewis et al. 2018; Jordan et al. 2018; Toropova et al. 2019). The p.Q1369R residue is likely surface-exposed or mediates dimerization via helix–helix interactions. We hypothesize that mutation of the positively charged arginine residue could destabilize the interaction, leading to disruption of functional dynein complexes; the mechanism by which such disruption may affect protein function should be further investigated.

Our *n*-of-1 genetic approach supports further research of the involvement of *DYNCH1H1* in ALS, in alignment with previous directions (MacArthur et al. 2014). Nonetheless, several limitations should be considered. First, the contribution of environmental factors affecting the penetrance of disease phenotype and the potential for underdiagnosing or misdiagnosing another disease with ALS cannot be excluded (Belbasis et al. 2016; Kuuluvainen et al. 2019). Second, our observations are limited to a single patient, which limits generalization and statistically driven conclusions (Kaszkin-Bettag and Hildebrandt 2012; Kiene et al. 2013). Genetic association studies in ALS patients from broader populations would be required. Third, our analysis of the identified pathogenic variants was based on in silico methods and requires further validation in experimental models harboring this *DYNC1H1* pathogenic variant; to our knowledge, none has been established to date. Fourth, our gene-centric approach excluded variants with currently unknown association with ALS (Supplemental Tables S3 and S4). Moreover, in the absence of information regarding parental family history such as the age to which the parents or earlier generations lived, ALS diagnoses or predispositions in the extended family, or nonpaternity limited our ability to distinguish between de novo and inherited modalities. As a result, no segregation data is presented that would provide definite evidence of the pathogenicity of *DYNC1H1* variant. Last, the identification of additional variants in the same patient is not necessarily indicative of an oligogenic inheritance. Collectively, larger studies would be needed before establishing a causal role of *DYNC1H1* variants in ALS etiology.

WES is also prone to certain limitations: (a) there are protein-coding regions (exome) where coverage may be less than sufficient; (b) it is inherently difficult to study noncoding, disease-causing variants (Claussnitzer et al. 2015); (c) large-scale structural variants (e.g., copy-number variations), more identifiable by long-read-base single-molecule sequencing (Audano et al. 2019), may not have been identified in our experiments; and (d) the possibility of false-positive results cannot be excluded. Another limitation is that, although we undertook many computational calculations to verify the identified variant as a bona fide variant, our results were not confirmed by Sanger sequencing. Nonetheless, the possibility for artifact is low, because the variant displayed a high sequencing depth in WES; hence, we would have otherwise detected some inconsistency among reads.

Despite the above limitations, our study prompts ALS specialists and researchers to further examine *DYNC1H1* p.Q1369R as a potential variant contributing to the genetic basis of ALS. Our data could reflect a variant whose reduced penetrance may necessitate the presence of additional genetic factors as contributors to the yet heterogenous basis of nonfamilial ALS.

METHODS

The patient was diagnosed and treated in the Neurology clinic of University Hospital of Thessaly, Larissa. The study received ethical approval by the University of Thessaly Hospital. Laboratory, neurophysiological, clinical, and other patient-related diagnostic assessments were performed using standard protocols. Extraction of genomic DNA was based on EDTA-treated blood samples collected as previously described (Siokas et al. 2020) following informed consent.

In Silico Analyses

Variant Quality Control, Damage Scores, and Conservation Scores

The bam file was indexed using SAMtools software (Li et al. 2009), and the candidate variant was visualized by IGV version 2.4.3.

To assess whether the *DYNC1H1*variant, as well as previously reported variants, was likely to cause any damage to protein function, we extracted the following damage scores: (a) SIFT (Ng and Henikoff 2003), (b) PolyPhen-2 (Adzhubei et al. 2010), (c) MutAss (Mutation Assessor score) (Reva et al. 2011), (d) Condel (González-Pérez and López-Bigas 2011), (e) CADD2 (Combined Annotation Dependent Depletion-2) (Kircher et al. 2014), and (f) Eigen (Ionita-Laza et al. 2016). For all scores except SIFT, larger scores correspond to a greater predicted damage.

To assess sequence conservation, we extracted conservation scores by three methods: (a) PhastCons (Ramani et al. 2019), (b) PhyloP (Ramani et al. 2019), and (c) GERP++ (Davydov et al. 2010). Additionally, we retrieved PhastCons and PhyloP scores for three levels of conservation—that is, vertebrates, placental mammals, and primates. For all conservation scores, the greater value corresponds to greater conservation.

For comparing *DYNC1H1* variants, we first extracted a range of damage prediction scores for each variant and ranked variants according to their expected functional impact based on multiple features. Then, we extracted a range of conservation scores and ranked variants from the most to the least conserved.

Assessment of Variant Effects on miRNA Recognition Sites and Transcription Factor Binding

To assess the possible effects of *DYNC1H1* variant on miRNA recognition sites, we queried the miRcode database (Jeggari et al. 2012), covering atypical transcript regions, such as the

5′ UTR and coding sequence, and limited our search space to miRNA targets within the coding regions of *DYNC1H1*.

To evaluate whether the variant overlapped or/and disrupted a known TFBS, the surrounding sequence was used to query the transcription factor motif database using the FIMO tool from the MEME suite (Grant et al. 2011). The potential disruption to the motif was estimated as a $\log_2$ ratio of reference and alternate allele frequencies in the motif position frequency matrix.

Structural Assessments

We applied MUpro (Cheng et al. 2006) and I-Mutant2.0 tools (Capriotti et al. 2005) to predict the effects of *DYNC1H1* variant on protein stability. The protein sequence for DYNC1H1 used as input was obtained from the NCBI Protein database (accession number: NP_001367.2). MUpro produces two sets of results: the first approach uses the Support Vector Machine (SVM) algorithm on the full protein sequence to predict both value and sign of energy change, and the second uses either the SVM or Neural Network on a smaller sequence window to predict the direction (sign) of energy change. Mutant2.0 tool complements the MUpro analysis, as it applies an SVM algorithm to predict protein stability changes by a single pathogenic variant. Similar to MUpro, I-Mutant runs in two modalities to either predict the direction of the free energy change or the magnitude of free energy change value, with positive values reflecting increased protein stability and negative ones corresponding to decreased stability.

We also used STRUM (Quan et al. 2016) for in silico determination of DYNC1H1 protein structural changes. Given that the structure prediction step is limited to a maximum protein length of 1500 amino acids, we used a 1500-amino acid window centered on the mutated residue as input sequence.

To generate a homology model of the mutant protein, we used Phyre2 (Kelley et al. 2015) in both normal and intensive modes, using as input the first 3500 amino acids of DYNC1H1, including the amino-terminal part and part of the motor domain.

We also performed molecular dynamics modeling using Molecular Operating Environment (MOE). The template crystal structures for homology modeling were selected based on amino acid sequence identity (56% PDB ID: 3VKH) and the structures' resolution cutoff (<3.8 Å). The MOE homology model method was used to model regions that were structurally available (for a comparative description of relevant software, see Nayeem et al. 2006). Ab initio modeling was also used for the part of the protein that could not be captured by homology modeling. Energy minimization for all four models was performed in MOE using the CHARMM27 force field, with root-mean-square deviation gradient set to 0.0001 Kcal/mol/Å^2 to remove the geometrical strain. The models were solvated with simple point charge (SPC) water using the truncated octahedron box extending 7 Å from each model. Molecular dynamics simulation was performed using the NVT ensemble (number of atoms, volume, and temperature remain constant) at 300 K, 1 atm, and 2-fsec step size for a total of 10 nsec. The whole system was solvated in explicit SPC water periodic systems. The results were analyzed in the MOE database.

ADDITIONAL INFORMATION

Data Deposition and Access

We note that a restriction has been imposed on genomic data deposition and release, because of lack of patient consent for making the sequence data publicly deposited,

available, and/or distributed. The variant was submitted to ClinVar (https://www.ncbi.nlm.nih.gov/clinvar/) and can be found under accession number SCV001774874.1.

Ethics Statement

The present study was performed according to the Declaration of Helsinki (as amended in its 7th version, 2013). Written informed consent from the patient was obtained prior to performing these genomic studies. Ethics permission was obtained from the University of Thessaly Hospital Ethic committee. Every effort was made to protect the identity of the patient.

Acknowledgments

Warm thanks are due to the patient's family. Also, many thanks are expressed by A.-F.A.M. to Anna S. Gkika for her continuous support in this study and to Dr. Maritina Sergaki for her critical comments on reading this manuscript. The authors are, also, indebted, regardless of order of mentioning below, to Dr. Bryan Traynor (National Institutes of Health) and to Drs. Elizabeth Fisher and Giampietro Schiavo (University College London) for conceptual discussions, Dr. Aliaksei Z. Holik for critical input and discussions on dry-lab approaches, Dr. George Z. Mentis (Columbia University) for discussion on ALS mouse models, Dr. Erika Holzbaur (University of Pennsylvania) for her insight on differential diagnosis with Perry Syndrome, to Dr. Simon Bullock and Dr. Clinton Lau (MRC Laboratory of Molecular Biology) for input on the structural aspects of DYNC1H1, to Dr. Steven Markus (Colorado State University) for feedback on yeast dynein equivalent, to Dr. Duyang Kim (Center for Genomics of Neurodegenerative Disease, New York Genome Center) for discussions on ALS variants, and to Dr. Eran Perlson and Mike Fainzilber (Weizmann Institute of Science) for discussions on *DYNC1H1*-related wet-lab approaches.

Author Contributions

A.-F.A.M., I.Z., G.P.P., G.P.C., and E.D. conceptualized the project; A.-F.A.M., D.V., E.P., and I.Z. curated the data; A.-F.A.M., D.V., E.P., and I.Z. performed the formal analyses; A.-F.A.M., I.Z., and E.D. acquired funding; A.-F.A.M., and E.D. led the investigation; A.-F.A.M., D.V., E.P., I.Z., G.P.C., and E.D. established the methodology; E.D. administered the project; A.-F.A.M., D.V., and G.P.C. visualized and wrote the original draft; A.-F.A.M., D.V., E.P., I.Z., G.P.P., G.P.C., and E.D. wrote, reviewed, and edited the article.

Funding

A.-F.A.M. was supported by an education scholarship through the Alexander Onassis Public Benefit Foundation, which played no role in the concept, study design, execution, or/and writing of this study and/or the collection, analysis, and interpretation of data, the decision to submit the article for publication, and any kind of financial aid for the coverage of publication costs. G.P.P. and E.D. are supported by the Greek National Precision Medicine Network for Neurodegenerative Diseases.

Competing Interest Statement

The authors have declared no competing interest.

Received March 23, 2021; accepted in revised form June 17, 2021.

REFERENCES

Abramzon YA, Fratta P, Traynor BJ, Chia R. 2020. The overlapping genetics of amyotrophic lateral sclerosis and frontotemporal dementia. *Front Neurosci* **14:** 42. doi:10.3389/fnins.2020.00042

Adzhubei IA, Schmidt S, Peshkin L, Ramensky VE, Gerasimova A, Bork P, Kondrashov AS, Sunyaev SR. 2010. A method and server for predicting damaging missense mutations. *Nat Methods* **7:** 248–249. doi:10.1038/nmeth0410-248

Al-Chalabi A, Calvo A, Chio A, Colville S, Ellis CM, Hardiman O, Heverin M, Howard RS, Huisman MHB, Keren N, et al. 2014. Analysis of amyotrophic lateral sclerosis as a multistep process: a population-based modelling study. *Lancet Neurol* **13:** 1108–1113. doi:10.1016/S1474-4422(14)70219-4

Al-Chalabi A, van den Berg LH, Veldink J. 2017. Gene discovery in amyotrophic lateral sclerosis: implications for clinical management. *Nat Rev Neurol* **13:** 96. doi:10.1038/nrneurol.2016.182

Amabile S, Jeffries L, McGrath JM, Ji W, Spencer-Manzon M, Zhang H, Lakhani SA. 2020. *DYNC1H1*-related disorders: a description of four new unrelated patients and a comprehensive review of previously reported variants. *Am J Med Genet A* **182:** 2049–2057. doi:10.1002/ajmg.a.61729

Ambrosini G, Vorontsov I, Penzar D, Groux R, Fornes O, Nikolaeva DD, Ballester B, Grau J, Grosse I, Makeev V, et al. 2020. Insights gained from a comprehensive all-against-all transcription factor binding motif benchmarking study. *Genome Biol* **21:** 1–18. doi:10.1186/s13059-020-01996-3

Andrés-Benito P, Povedano M, Torres P, Portero-Otin M, Ferrer I. 2019. Altered dynein axonemal assembly factor 1 expression in C-boutons in bulbar and spinal cord motor-neurons in sporadic amyotrophic lateral sclerosis. *J Neuropathol Exp Neurol* **78:** 416–425. doi:10.1093/jnen/nlz019

Arthur KC, Calvo A, Price TR, Geiger JT, Chiò A, Traynor BJ. 2016. Projected increase in amyotrophic lateral sclerosis from 2015 to 2040. *Nat Commun* **7:** 12408. doi:10.1038/ncomms12408

Audano PA, Sulovari A, Graves-Lindsay TA, Cantsilieris S, Sorensen M, Welch AE, Dougherty ML, Nelson BJ, Shah A, Dutcher SK, et al. 2019. Characterizing the major structural variant alleles of the human genome. *Cell* **176:** 663–675.e619. doi:10.1016/j.cell.2018.12.019

Ayalew M, Le-Niculescu H, Levey D, Jain N, Changala B, Patel S, Winiger E, Breier A, Shekhar A, Amdur R, et al. 2012. Convergent functional genomics of schizophrenia: from comprehensive understanding to genetic risk prediction. *Mol Psychiatry* **17:** 887–905. doi:10.1038/mp.2012.37

Bandres-Ciga S, Noyce AJ, Hemani G, Nicolas A, Calvo A, Mora G, Tienari PJ, Stone DJ, Nalls MA, Singleton AB, et al. 2019. Shared polygenic risk and causal inferences in amyotrophic lateral sclerosis. *Ann Neurol* **85:** 470–481. doi:10.1002/ana.25431

Becker L-L, Dafsari HS, Schallner J, Abdin D, Seifert M, Petit F, Smol T, Bok L, Rodan L, Krapels I, et al. 2020. The clinical-phenotype continuum in *DYNC1H1*-related disorders—genomic profiling and proposal for a novel classification. *J Hum Genet* **65:** 1003–1017. doi:10.1038/s10038-020-0803-1

Belbasis L, Bellou V, Evangelou E. 2016. Environmental risk factors and amyotrophic lateral sclerosis: an umbrella review and critical assessment of current evidence from systematic reviews and meta-analyses of observational studies. *Neuroepidemiology* **46:** 96–105. doi:10.1159/000443146

Bercier V, Hubbard JM, Fidelin K, Duroure K, Auer TO, Revenu C, Wyart C, Del Bene F. 2019. Dynactin1 depletion leads to neuromuscular synapse instability and functional abnormalities. *Mol Neurodegener* **14:** 27. doi:10.1186/s13024-019-0327-3

Cady J, Allred P, Bali T, Pestronk A, Goate A, Miller TM, Mitra RD, Ravits J, Harms MB, Baloh RH. 2015. Amyotrophic lateral sclerosis onset is influenced by the burden of rare variants in known amyotrophic lateral sclerosis genes. *Ann Neurol* **77:** 100–113. doi:10.1002/ana.24306

Capriotti E, Fariselli P, Casadio R. 2005. I-Mutant2.0: predicting stability changes upon mutation from the protein sequence or structure. *Nucleic Acids Res* **33:** W306–W310. doi:10.1093/nar/gki375

Carvalho MD, Swash M. 2009. Awaji diagnostic algorithm increases sensitivity of El Escorial criteria for ALS diagnosis. *Amyotroph Lateral Scler* **10:** 53–57. doi:10.1080/17482960802521126

Chen S, Sayana P, Zhang X, Le W. 2013. Genetics of amyotrophic lateral sclerosis: an update. *Mol Neurodegener* **8:** 28. doi:10.1186/1750-1326-8-28

Cheng J, Randall A, Baldi P. 2006. Prediction of protein stability changes for single-site mutations using support vector machines. *Proteins* **62:** 1125–1132. doi:10.1002/prot.20810

Chia R, Chio A, Traynor BJ. 2018. Novel genes associated with amyotrophic lateral sclerosis: diagnostic and clinical implications. *Lancet Neurol* **17:** 94–102. doi:10.1016/S1474-4422(17)30401-5

Claussnitzer M, Dankel SN, Kim K-H, Quon G, Meuleman W, Haugen C, Glunk V, Sousa IS, Beaudry JL, Puviindran V, et al. 2015. FTO Obesity variant circuitry and adipocyte browning in humans. *N Engl J Med* **373:** 895–907. doi:10.1056/NEJMoa1502214

Connolly S, Galvin M, Hardiman O. 2015. End-of-life management in patients with amyotrophic lateral sclerosis. *Lancet Neurol* **14:** 435–442. doi:10.1016/S1474-4422(14)70221-2

Corrado L, Mazzini L, Oggioni GD, Luciano B, Godi M, Brusco A, D'Alfonso S. 2011. *ATXN-2* CAG repeat expansions are interrupted in ALS patients. *Hum Genet* **130:** 575–580. doi:10.1007/s00439-011-1000-2

Courchesne SL, Pazyra-Murphy MF, Lee DJ, Segal RA. 2011. Neuromuscular junction defects in mice with mutation of *dynein heavy chain 1*. *PLoS One* **6:** e16753. doi:10.1371/journal.pone.0016753

Davydov EV, Goode DL, Sirota M, Cooper GM, Sidow A, Batzoglou S. 2010. Identifying a high fraction of the human genome to be under selective constraint using GERP++. *PLoS Comput Biol* **6:** e1001025. doi:10.1371/journal.pcbi.1001025

de Vries BS, Rustemeijer LMM, Bakker LA, Schröder CD, Veldink JH, van den Berg LH, Nijboer TCW, van Es MA. 2019. Cognitive and behavioural changes in PLS and PMA: challenging the concept of restricted phenotypes. *J Neurol Neurosurg Psychiatry* **90:** 141–147. doi:10.1136/jnnp-2018-318788

Dror RO, Dirks RM, Grossman J, Xu H, Shaw DE. 2012. Biomolecular simulation: a computational microscope for molecular biology. *Annu Rev Biophys* **41:** 429–452. doi:10.1146/annurev-biophys-042910-155245

Ewing B, Green P. 1998. Base-calling of automated sequencer traces using *phred*. II. Error probabilities. *Genome Res* **8:** 186–194. doi:10.1101/gr.8.3.186

Fergani A, Eschbach J, Oudart H, Larmet Y, Schwalenstocker B, Ludolph AC, Loeffler J-P, Dupuis L. 2011. A mutation in the dynein heavy chain gene compensates for energy deficit of mutant SOD1 mice and increases potentially neuroprotective IGF-1. *Mol Neurodegener* **6:** 26. doi:10.1186/1750-1326-6-26

Galdadas I, Gervasio FL, Cournia Z. 2020. Unravelling the effect of the E545K mutation on PI3Kα kinase. *Chem Sci* **11:** 3511–3515. doi:10.1039/C9SC05903B

Garrett CA, Barri M, Kuta A, Soura V, Deng W, Fisher EM, Schiavo G, Hafezparast M. 2014. *DYNC1H1* mutation alters transport kinetics and ERK1/2-cFos signalling in a mouse model of distal spinal muscular atrophy. *Brain* **137:** 1883–1893. doi:10.1093/brain/awu097

González-Pérez A, López-Bigas N. 2011. Improving the assessment of the outcome of nonsynonymous SNVs with a consensus deleteriousness score, Condel. *Am J Hum Genet* **88:** 440–449. doi:10.1016/j.ajhg.2011.03.004

Goulielmos GN, Zervou MI, Eliopoulos E. 2019. Functional significance of the C324R mutation examined using a structural biological approach. *J Rheumatol* **46:** 654–655. doi:10.3899/jrheum.181346

Grant CE, Bailey TL, Noble WS. 2011. FIMO: scanning for occurrences of a given motif. *Bioinformatics* **27:** 1017–1018. doi:10.1093/bioinformatics/btr064

Hafezparast M, Klocke R, Ruhrberg C, Marquardt A, Ahmad-Annuar A, Bowen S, Lalli G, Witherden AS, Hummerich H, Nicholson S, et al. 2003. Mutations in dynein link motor neuron degeneration to defects in retrograde transport. *Science* **300:** 808–812. doi:10.1126/science.1083129

Hardiman O, Al-Chalabi A, Chio A, Corr EM, Logroscino G, Robberecht W, Shaw PJ, Simmons Z, van den Berg LH. 2017. Amyotrophic lateral sclerosis. *Nat Rev Dis Primers* **3:** 17071. doi:10.1038/nrdp.2017.71

Harms MB, Ori-McKenney KM, Scoto M, Tuck EP, Bell S, Ma D, Masi S, Allred P, Al-Lozi M, Reilly MM, et al. 2012. Mutations in the tail domain of *DYNC1H1* cause dominant spinal muscular atrophy. *Neurology* **78:** 1714–1720. doi:10.1212/WNL.0b013e3182556c05

Helferich AM, Brockmann SJ, Reinders J, Deshpande D, Holzmann K, Brenner D, Andersen PM, Petri S, Thal DR, Michaelis J, et al. 2018. Dysregulation of a novel miR-1825/TBCB/TUBA4A pathway in sporadic and familial ALS. *Cell Mol Life Sci* **75:** 4301–4319. doi:10.1007/s00018-018-2873-1

Hoang HT, Schlager MA, Carter AP, Bullock SL. 2017. DYNC1H1 mutations associated with neurological diseases compromise processivity of dynein-dynactin-cargo adaptor complexes. *Proc Natl Acad Sci* **114:** E1597–E1606. doi:10.1073/pnas.1620141114

Ionita-Laza I, McCallum K, Xu B, Buxbaum JD. 2016. A spectral approach integrating functional genomic annotations for coding and noncoding variants. *Nat Genet* **48:** 214. doi:10.1038/ng.3477

Jeggari A, Marks DS, Larsson E. 2012. miRcode: a map of putative microRNA target sites in the long non-coding transcriptome. *Bioinformatics* **28:** 2062–2063. doi:10.1093/bioinformatics/bts344

Jordan MA, Diener DR, Stepanek L, Pigino G. 2018. The cryo-EM structure of intraflagellar transport trains reveals how dynein is inactivated to ensure unidirectional anterograde movement in cilia. *Nat Cell Biol* **20:** 1250–1255. doi:10.1038/s41556-018-0213-1

Kapeli K, Martinez FJ, Yeo GW. 2017. Genetic mutations in RNA-binding proteins and their roles in ALS. *Hum Genet* **136:** 1193–1214. doi:10.1007/s00439-017-1830-7

Kaszkin-Bettag M, Hildebrandt W. 2012. Case reports on cancer therapies: the urgent need to improve the reporting quality. *Glob Adv Health Med* **1:** 8–10. doi:10.7453/gahmj.2012.1.2.002

Kelley LA, Mezulis S, Yates CM, Wass MN, Sternberg MJE. 2015. The Phyre2 web portal for protein modeling, prediction and analysis. *Nat Protoc* **10:** 845–858. doi:10.1038/nprot.2015.053

Kenna KP, McLaughlin RL, Byrne S, Elamin M, Heverin M, Kenny EM, Cormican P, Morris DW, Donaghy CG, Bradley DG, et al. 2013. Delineating the genetic heterogeneity of ALS using targeted high-throughput sequencing. *J Med Genet* **50:** 776–783. doi:10.1136/jmedgenet-2013-101795

Keogh MJ, Wei W, Aryaman J, Wilson I, Talbot K, Turner MR, McKenzie CA, Troakes C, Attems J, Smith C, et al. 2018. Oligogenic genetic variation of neurodegenerative disease genes in 980 postmortem human brains. *J Neurol Neurosurg Psychiatry* **89:** 813–816. doi:10.1136/jnnp-2017-317234

Kiene H, Hamre HJ, Kienle GS. 2013. In support of clinical case reports: a system of causality assessment. *Glob Adv Health Med* **2:** 64–75. doi:10.7453/gahmj.2012.061

Kircher M, Witten DM, Jain P, O'Roak BJ, Cooper GM, Shendure J. 2014. A general framework for estimating the relative pathogenicity of human genetic variants. *Nat Genet* **46:** 310–315. doi:10.1038/ng.2892

Koushika SP, Schaefer AM, Vincent R, Willis JH, Bowerman B, Nonet ML. 2004. Mutations in *Caenorhabditis elegans* cytoplasmic dynein components reveal specificity of neuronal retrograde cargo. *J Neurosci* **24:** 3907–3916. doi:10.1523/JNEUROSCI.5039-03.2004

Kulakovskiy IV, Vorontsov IE, Yevshin IS, Soboleva AV, Kasianov AS, Ashoor H, Ba-Alawi W, Bajic VB, Medvedeva YA, Kolpakov FA, et al. 2016. HOCOMOCO: expansion and enhancement of the collection of transcription factor binding sites models. *Nucleic Acids Res* **44:** D116–D125. doi:10.1093/nar/gkv1249

Kuuluvainen L, Kaivola K, Mönkäre S, Laaksovirta H, Jokela M, Udd B, Valori M, Pasanen P, Paetau A, Traynor BJ. 2019. Oligogenic basis of sporadic ALS: the example of *SOD1* p. Ala90Val mutation. *Neurol Genet* **5:** e335. doi:10.1212/NXG.0000000000000335

LaMonte BH, Wallace KE, Holloway BA, Shelly SS, Ascaño J, Tokito M, Van Winkle T, Howland DS, Holzbaur EL. 2002. Disruption of dynein/dynactin inhibits axonal transport in motor neurons causing late-onset progressive degeneration. *Neuron* **34:** 715–727. doi:10.1016/S0896-6273(02)00696-7

Lattante S, Doronzio PN, Marangi G, Conte A, Bisogni G, Bernardo D, Russo T, Lamberti D, Patrizi S, Apollo FP, et al. 2019. Coexistence of variants in *TBK1* and in other ALS-related genes elucidates an oligogenic model of pathogenesis in sporadic ALS. *Neurobiol Aging* **84:** 239.e239–239.e214. doi:10.1016/j.neurobiolaging.2019.03.010

Lesgidou N, Eliopoulos E, Goulielmos GN, Vlassi M. 2018. Insights on the alteration of functionality of a tyrosine kinase 2 variant: a molecular dynamics study. *Bioinformatics* **34:** i781–i786. doi:10.1093/bioinformatics/bty556

Lewis TR, Zareba M, Link BA, Besharse JC. 2018. Cone myoid elongation involves unidirectional microtubule movement mediated by dynein-1. *Mol Biol Cell* **29:** 180–190. doi:10.1091/mbc.E17-08-0525

Li H, Handsaker B, Wysoker A, Fennell T, Ruan J, Homer N, Marth G, Abecasis G, Durbin R, et al. 2009. The Sequence Alignment/Map format and SAMtools. *Bioinformatics* **25:** 2078–2079. doi:10.1093/bioinformatics/btp352

MacArthur D, Manolio T, Dimmock D, Rehm H, Shendure J, Abecasis G, Adams D, Altman R, Antonarakis S, Ashley E, et al. 2014. Guidelines for investigating causality of sequence variants in human disease. *Nature* **508:** 469–476. doi:10.1038/nature13127

Marzo MG, Griswold JM, Ruff KM, Buchmeier RE, Fees CP, Markus SM. 2019. Molecular basis for dyneinopathies reveals insight into dynein regulation and dysfunction. *Elife* **8:** e47246. doi:10.7554/eLife.47246

McCann EP, Henden L, Fifita JA, Zhang KY, Grima N, Bauer DC, Chan Moi Fat S, Twine NA, Pamphlett R, Kiernan MC, et al. 2021. Evidence for polygenic and oligogenic basis of Australian sporadic amyotrophic lateral sclerosis. *J Med Genet* **58:** 87–95. doi:10.1136/jmedgenet-2020-106866

McKenna A, Hanna M, Banks E, Sivachenko A, Cibulskis K, Kernytsky A, Garimella K, Altshuler D, Gabriel S, Daly M. 2010. The genome analysis toolkit: a MapReduce framework for analyzing next-generation DNA sequencing data. *Genome Res* **20:** 1297–1303. doi:10.1101/gr.107524.110

Mishima T, Fujioka S, Tomiyama H, Yabe I, Kurisaki R, Fujii N, Neshige R, Ross OA, Farrer MJ, Dickson DW, et al. 2018. Establishing diagnostic criteria for Perry syndrome. *J Neurol Neurosurg Psychiatry* **89:** 482–487. doi:10.1136/jnnp-2017-316864

Moore JK, Sept D, Cooper JA. 2009. Neurodegeneration mutations in dynactin impair dynein-dependent nuclear migration. *Proc Natl Acad Sci* **106:** 5147–5152. doi:10.1073/pnas.0810828106

Nayeem A, Sitkoff D, Krystek Jr S. 2006. A comparative study of available software for high-accuracy homology modeling: from sequence alignments to structural models. *Protein Sci* **15:** 808–824. doi:10.1110/ps.051892906

Ng PC, Henikoff S. 2003. SIFT: predicting amino acid changes that affect protein function. *Nucleic Acids Res* **31:** 3812–3814. doi:10.1093/nar/gkg509

Niu Q, Wang X, Shi M, Jin Q. 2015. A novel *DYNC1H1* mutation causing spinal muscular atrophy with lower extremity predominance. *Neurol Genet* **1:** e20. doi:10.1212/NXG.0000000000000017

Oiwa K, Sakakibara H. 2005. Recent progress in dynein structure and mechanism. *Curr Opin Cell Biol* **17:** 98–103. doi:10.1016/j.ceb.2004.12.006

Pampalakis G, Mitropoulos K, Xiromerisiou G, Dardiotis E, Deretzi G, Anagnostouli M, Katsila T, Rentzos M, Patrinos GP. 2019. New molecular diagnostic trends and biomarkers for amyotrophic lateral sclerosis. *Hum Mutat* **40:** 361–373. doi:10.1002/humu.23697

Peeters K, Bervoets S, Chamova T, Litvinenko I, De Vriendt E, Bichev S, Kancheva D, Mitev V, Kennerson M, Timmerman V, et al. 2015. Novel mutations in the *DYNC1H1* tail domain refine the genetic and clinical spectrum of dyneinopathies. *Hum Mutat* **36:** 287–291. doi:10.1002/humu.22744

Quan L, Lv Q, Zhang Y. 2016. STRUM: structure-based prediction of protein stability changes upon single-point mutation. *Bioinformatics* **32:** 2936–2946. doi:10.1093/bioinformatics/btw361

Ramani R, Krumholz K, Huang Y-F, Siepel A. 2019. PhastWeb: a web interface for evolutionary conservation scoring of multiple sequence alignments using PhastCons and PhyloP. *Bioinformatics* **35:** 2320–2322. doi:10.1093/bioinformatics/bty966

Reva B, Antipin Y, Sander C. 2011. Predicting the functional impact of protein mutations: application to cancer genomics. *Nucleic Acids Res* **39:** e118. doi:10.1093/nar/gkr407

Richards S, Aziz N, Bale S, Bick D, Das S, Gastier-Foster J, Grody WW, Hegde M, Lyon E, Spector E, et al. 2015. Standards and guidelines for the interpretation of sequence variants: a joint consensus recommendation of the American College of Medical Genetics and Genomics and the Association for Molecular Pathology. *Genet Med* **17:** 405–423. doi:10.1038/gim.2015.30

Rooney JP, Brayne C, Tobin K, Logroscino G, Glymour MM, Hardiman O. 2017. Benefits, pitfalls, and future design of population-based registers in neurodegenerative disease. *Neurology* **88:** 2321–2329. doi:10.1212/WNL.0000000000004038

Sandelin A, Alkema W, Engström P, Wasserman WW, Lenhard B. 2004. JASPAR: an open-access database for eukaryotic transcription factor binding profiles. *Nucleic Acids Res* **32:** D91–D94. doi:10.1093/nar/gkh012

Scarlino S, Domi T, Pozzi L, Romano A, Pipitone GB, Falzone YM, Mosca L, Penco S, Lunetta C, Sansone V. 2020. Burden of rare variants in ALS and axonal hereditary neuropathy genes influence survival in ALS: insights from a next generation sequencing study of an Italian ALS cohort. *Int J Mol Sci* **21:** 3346. doi:10.3390/ijms21093346

Scoto M, Rossor AM, Harms MB, Cirak S, Calissano M, Robb S, Manzur AY, Martínez Arroyo A, Rodriguez Sanz A, Mansour S, et al. 2015. Novel mutations expand the clinical spectrum of *DYNC1H1*-associated spinal muscular atrophy. *Neurology* **84:** 668–679. doi:10.1212/WNL.0000000000001269

Shah PR, Ahmad-Annuar A, Ahmadi KR, Russ C, Sapp PC, Robert Horvitz H, Brown Jr RH, Goldstein DB, Fisher EM. 2006. No association of *DYNC1H1* with sporadic ALS in a case-control study of a northern European derived population: a tagging SNP approach. *Amyotroph Lateral Scler* **7:** 46–56. doi:10.1080/14660820500397057

Siokas V, Karampinis E, Aloizou AM, Mentis AA, Liakos P, Papadimitriou D, Liampas I, Nasios G, Bogdanos DP, Hadjigeorgiou GM, et al. 2020. *CYP1A2* rs762551 polymorphism and risk for amyotrophic lateral sclerosis. *Neurol Sci* **42:** 175–182. doi:10.1007/s10072-020-04535-x

Sokratous M, Lucia S, Bourinaris T, Marogianni C, Arnaoutoglou M, Patrikiou E, Ralli S, Markou A, Dardiotis E, Houlden H, et al. 2020. Prevalence of *C9orf72* hexanucleotide repeat expansion in Greek patients with sporadic ALS. *Amyotroph Lateral Scler Frontotemporal Degener* **21:** 470–472. doi:10.1080/21678421.2020.1757115

Stergachis AB, Haugen E, Shafer A, Fu W, Vernot B, Reynolds A, Raubitschek A, Ziegler S, LeProust EM, Akey JM, et al. 2013. Exonic transcription factor binding directs codon choice and affects protein evolution. *Science* **342:** 1367–1372. doi:10.1126/science.1243490

Talbot K, Feneberg E, Scaber J, Thompson AG, Turner MR. 2018. Amyotrophic lateral sclerosis: the complex path to precision medicine. *J Neurol* **265:** 2454–2462. doi:10.1007/s00415-018-8983-8

Talkowski ME, Rosenfeld JA, Blumenthal I, Pillalamarri V, Chiang C, Heilbut A, Ernst C, Hanscom C, Rossin E, Lindgren AM, et al. 2012. Sequencing chromosomal abnormalities reveals neurodevelopmental loci that confer risk across diagnostic boundaries. *Cell* **149:** 525–537. doi:10.1016/j.cell.2012.03.028

Toropova K, Zalyte R, Mukhopadhyay AG, Mladenov M, Carter AP, Roberts AJ. 2019. Structure of the dynein-2 complex and its assembly with intraflagellar transport trains. *Nat Struct Mol Biol* **26:** 823–829. doi:10.1038/s41594-019-0286-y

Tripolszki K, Gampawar P, Schmidt H, Nagy ZF, Nagy D, Klivényi P, Engelhardt JI, Széll M. 2019. Comprehensive genetic analysis of a Hungarian amyotrophic lateral sclerosis cohort. *Front Genet* **10:** 732. doi:10.3389/fgene.2019.00732

Tsai M-J, Hsu C-Y, Sheu C-C. 2017. Amyotrophic lateral sclerosis. *N Engl J Med* **377:** 1602. doi:10.1056/NEJMc1710379

Tsurusaki Y, Saitoh S, Tomizawa K, Sudo A, Asahina N, Shiraishi H, Ito J, Tanaka H, Doi H, Saitsu H, et al. 2012. A *DYNC1H1* mutation causes a dominant spinal muscular atrophy with lower extremity predominance. *Neurogenetics* **13:** 327–332. doi:10.1007/s10048-012-0337-6

Viollet LM, Swoboda KJ, Mao R, Best H, Ha Y, Toutain A, Guyant-Marechal L, Laroche-Raynaud C, Ghorab K, Barthez MA, et al. 2020. A novel pathogenic variant in *DYNC1H1* causes various upper and lower motor neuron anomalies. *Eur J Med Genet* **63:** 104063. doi:10.1016/j.ejmg.2020.104063

Vlachakis D. 2009. Theoretical study of the Usutu virus helicase 3D structure, by means of computer-aided homology modelling. *Theor Biol Med Model* **6:** 9. doi:10.1186/1742-4682-6-9

Wegorzewska I, Bell S, Cairns NJ, Miller TM, Baloh RH. 2009. TDP-43 mutant transgenic mice develop features of ALS and frontotemporal lobar degeneration. *Proc Natl Acad Sci* **106:** 18809–18814. doi:10.1073/pnas.0908767106